Metallothionein Isoform 3 as a Potential Biomarker for Human Bladder Cancer

Mary Ann Sens,[1] Seema Somji,[2] Donald L. Lamm,[2] Scott H. Garrett,[2] Frank Slovinsky,[1] John H. Todd,[1] and Donald A. Sens[2]

[1]Robert C. Byrd Health Sciences Center, Department of Pathology, [2]Department of Urology, West Virginia University, Morgantown, West Virginia, USA

The goal of the present study was to determine if the expression of metallothionein isoform 3 (MT-3) might serve as a biomarker for human bladder cancer. To accomplish this goal, we defined the localization and expression of MT-3 protein and mRNA using fresh and archival biopsy specimens obtained from patients undergoing differential diagnosis for a variety of bladder disorders. We used immunohistochemistry, immunoblot, and RT-PCR analysis to define the localization and expression of MT-3 protein and mRNA. Immunohistochemical analysis disclosed no immunoreactivity for MT-3 in normal bladder cells. The absence of MT-3 expression in the normal bladder was further confirmed by demonstrating that MT-3 mRNA could not be detected using reverse transcriptase-polymerase chain reaction (RT-PCR) or MT-3 protein using immunoblot. Immunohistochemistry also disclosed no immunoreactivity for MT-3 in archival biopsy specimens from patients with interstitial cystitis and related disorders. Immunohistochemical analysis demonstrated that MT-3 was expressed in carcinoma *in situ* (CIS), high-grade bladder cancer, low-grade bladder cancer, and dysplastic lesions. MT-3 immunostaining was intense in both CIS and high-grade bladder cancer, and low to moderate in low-grade bladder cancer and dysplastic lesions. We determined MT-3 mRNA expression in a subset of these bladder cancer specimens; expression was elevated as compared to that of the housekeeping gene, β-actin. The cDNA from the RT-PCR reaction primed for MT-3 contained a *Fok*I restriction site, a site unique for MT-3 as compared to other MT family members. In conclusion, this study demonstrates that MT-3 is up-regulated in human bladder cancer and that this up-regulation increases with increasing tumor grade. The finding that MT-3 expression is minimal in normal bladder suggests that MT-3 might be developed into an effective biomarker for bladder cancer. *Key words*: biomarker, bladder, bladder cancer, carcinoma *in situ*, cystitis, immunohistochemistry, inflammation, interstitial cystitis, metallothionein, RT-PCR, transitional cell carcinoma, urothelium. *Environ Health Perspect* 108:413–418 (2000). [Online 17 March 2000]
http://ehpnet1.niehs.nih.gov/docs/2000/108p413-418sens/abstract.html

The progress against bladder cancer over the last 20 years and the current diagnosis and treatment strategies for managing the disease have been the subject of recent reviews (*1,2*). In the United States over 54,000 new cases of bladder cancer are diagnosed each year and more than 12,000 annual deaths result from the disease (*3*). Bladder cancer is the fifth most common cancer in the United States, and approximately 15–30% of bladder tumors show grade and stage progression (*4*). Metastasis is the main cause of death in bladder cancer patients, and approximately 50% of patients who present with muscle-invasive bladder tumors die from metastatic disease (*5*). The number of cases of bladder cancer has increased each year for the past 20 years while the mortality attributed to the disease has remained relatively constant (*1*).

Epidemiologically, bladder cancer represents one of the first cancers in which environmental carcinogens were found to play the major role in causing the disease. In 1895, Rehn (*6*) observed an association between exposure to aromatic amines and bladder cancer in factory workers. This association was confirmed in both animal models and in humans working in industries that involved exposure to aromatic amines (*7,8*). Many studies have described an association between cigarette smoking and bladder cancer; some reports suggested a 2- to 4-fold increased risk and that 50% of the bladder cancers in men would not occur in the absence of cigarette smoking (*9,10*). The majority of the remaining bladder cancers are believed to be caused by industrial or agricultural carcinogens. The number of cigarettes smoked, degree of inhalation, type of tobacco, use of filters, and smoking cessation all have specific relationships to the development of bladder cancer (*11*). There are no widely accepted tumor markers that allow widespread screening for the early presence of bladder cancer or for the detection and monitoring of advanced metastatic disease; however, evidence suggests that such markers could impact on reducing the mortality of this disease [reviewed by Lamm (*1*) and Droller (*2*)].

The need for effective biomarkers for the detection of bladder cancer led us to define the expression of metallothionein isoform 3 (MT-3) in the normal and cancerous bladder. The rationale for this examination comes from recent findings showing that MT-3 is expressed in the epithelial components of both the normal kidney and prostate gland, with altered expression in organ-derived cancers (*12–14*). The finding of MT-3 expression in these organs was unexpected because the recently characterized *MT-3* gene was initially reported to have a highly restricted expression pattern confined to neural tissues (*15*). The finding that MT-3 was expressed in other tissues of the urogenital system motivated the expansion of this analysis to determine if MT-3 is expressed in the bladder, and if this expression is altered in epithelial cell-derived cancers.

Materials and Methods

Bladder specimens for immunohistochemical analysis of MT-3 expression. For the immunohistochemical analysis of MT-3 expression, we obtained biopsy tissues from paraffin blocks that originated from previously completed patient diagnostic procedures. These biopsy specimens are archived, after completion of diagnostic procedures, in the Department of Pathology of the West Virginia University Hospitals (Morgantown, WV). To define the immunohistochemical expression of MT-3 in control and noncancerous lesions of the bladder, we utilized a set of paraffin-embedded tissue samples that had been used previously to determine heat shock protein expression in the bladder of patients with interstitial cystitis (IC) and IC-like syndromes (*16–18*). This set of samples consisted of 7 specimens of control, nondiseased, adult bladder; 9 specimens from six adult patients with a diagnosis of cystitis; 11 specimens from nine adult patients with a diagnosis of IC; 6 specimens from three adult patients with a possible diagnosis of IC; and 6 specimens from adult patients with symptoms of cystitis after successful BCG (bacille Calmette-Guérin) therapy for transitional cell carcinoma (TCC). The nine cases of cystitis displayed varying degrees of inflammation, and three of the cases met histopathologic criteria for

Address correspondence to D.A. Sens, Department of Urology, West Virginia University, PO Box 9251, Morgantown, WV 26506-9251 USA. Telephone: (304) 293-3212. Fax: (304) 293-6249. E-mail: dsens@wvu.edu

Received 31 August 1999; accepted 12 November 1999.

follicular cystitis. In 10 of the adult specimens, multiple biopsies from different areas of the bladder were available. IC occurs predominantly in female patients and all IC samples were from females.

We determined the immunohistochemical expression of MT-3 in urothelial carcinoma of the bladder on paraffin-embedded archival tissue samples from 20 patients with a diagnosis of TCC of the bladder. These patients (13 males and 7 females) had all undergone treatment for bladder cancer with BCG therapy and most had undergone multiple bladder biopsies during the course of treatment. The average age was 62.4 at the time of diagnosis. At the time of initial diagnosis, 8 patients had biopsies demonstrating low-grade urothelial carcinoma (LG TCC) and 12 patients had high-grade urothelial carcinoma (HG TCC), 11 of which were proven by biopsy and one of which had positive cytology. The initial biopsies showed carcinoma *in situ* (CIS) in one patient with low-grade papillary urothelial carcinoma and in three patients with HG TCC. None of the patients demonstrated muscle invasion at the time of initial diagnosis; all were staged at Ta (*15*), T1 (*4*), or TIS (*1*). During the course of treatment, seven patients exhibited only low-grade recurrences; four patients had high-grade recurrences without histologically evident CIS; three patients had both high-grade and low-grade recurrences; one patient had low-grade papillary carcinoma with adjacent areas of CIS; three patients had high-grade carcinoma with areas of CIS; and one patient exhibited the full spectrum of urothelial cell carcinomas with sequential biopsies demonstrating high-grade carcinoma, low grade carcinoma, and CIS. There were a total of 92 biopsies on these patients; individual patients had between 1 and 20 biopsies in the course of treatment. From these 92 biopsies, we selected 55 specimens for immunohistochemical examination. For analysis of MT-3 expression, we subdivided the specimens into five categories. The benign category consisted of 33 observations from patients with TCCs that were histologically benign. Eleven of these sections were from patients who had other biopsies taken at the same time that revealed either LG TCC (five sections) or HG TCC (six sections) and 10 were from patients with TCC whose biopsies were negative but who were positive for TCC on other independent examinations. Twelve observations of benign urothelium came from sections with malignancy (nine LG TCC and three HG TCC) that had adjacent areas of histologically normal urothelium. The dysplasia included 18 observations from sections with malignancy that had adjacent areas histologically defined as being dysplastic using standard diagnostic criteria. The LG TCC category consisted of 23 observations from 21 biopsies obtained from 13 patients. The HG TCC category contained lesions defined by standard diagnostic criteria as HG TCC without histologically demonstrable areas of CIS. In this group, a total of 25 sections from 18 separate biopsies from 12 patients were available. The CIS category consisted of seven sections from six separate biopsies from six patients with areas that met standard diagnostic criteria for CIS. One biopsy demonstrated only CIS; four had concomitant HG TCC, and the remaining two had LG TCC. The degree of MT immunoreactivity was judged by two pathologists using a 0 to +4 scale, where 0 indicated negative immunoreactivity and +4 strong immunoreactivity. The slides used in the analysis were blinded for disease status by random numbering of the slides and these were decoded only after both pathologists had completed the evaluation of staining intensity.

Bladder specimens for analysis of MT-3 mRNA expression. To determine the MT-3 mRNA expression in control bladder, we used three independent samples of total RNA prepared from undiseased adult bladder from the previous studies on IC (*16–18*) and added three additional samples for the present analysis. These total RNA samples were prepared from six independent specimens of undiseased adult bladder obtained from biopsy or surgical specimens after the completion of diagnostic protocols. For the determination of MT-3 mRNA expression in TCC, we isolated total RNA from full-thickness (10 μm) sections from a subset of the paraffin-embedded tissues to determine the immunohistochemical expression of MT-3 in TCC. We chose samples where the malignant lesion made up over 85% of the section.

Immunohistochemical localization of MT-3. We generated the affinity purified antibody against human MT-3 using the dodecapeptide GGEAAEAEAEKC (corresponding to MT-3 amino acids 53–64, which contain the MT-3 unique amino acid insert) conjugated through the *C*-terminal cysteine SH group to keyhole limpet hemocyanine using maleimidobenzoyl-*N*-hydroxysuccinimide ester, as described previously (*13,14*). This antibody was used to immunize New Zealand white rabbits. The MT-3 antibody was affinity purified using the dodecapeptide linked to SulfoLink gel (Pierce, Rockford, IL) through the *C*-terminal cysteine residue. Archival bladder specimens were routinely fixed in 10% neutral buffered formalin for 16–18 hr. All tissues were transferred to 70% ethanol and dehydrated in 100% ethanol. Dehydrated tissues were cleared in xylene, infiltrated, and embedded in paraffin. We cut serial sections at 3–5 μm for use in immunohistochemical protocols. Before immunostaining, sections were pretreated in a microwave at 700 W in 10 mM citrate buffer (pH 6.0) for 5 min. The sections were allowed to cool for 5 min at room temperature, then microwaved again for 5 min and immersed into distilled water. The affinity purified primary anti-MT-3 antibody was localized using the avidin–biotin–peroxidase complex (ABC) procedure (BioGenex optimax immunostainer; BioGenex, Inc., San Ramon, CA) using diaminobenzidine for visualization (stable DAB; Research Genetics, Huntsville, AL). We rinsed the slides in distilled water, dehydrated them in solutions containing graded ethanol concentrations, cleared them in xylene, then placed coverslips on them. The negative controls consisted of omission of primary antibody from the immunohistochemical ABC sequence and abolishment of staining by titration of the primary antibody with the peptide used for immunization. The positive control used sections of human brain.

RNA isolation and RT-PCR analysis of MT-3 mRNA expression in normal bladder. We ground bladder tissue to a powder under liquid nitrogen and isolated total RNA from the powdered tissue according to the protocol supplied with TRI REAGENT (Molecular Research Center, Inc., Cincinnati, OH), as described previously (*19,20*). We determined the concentration and purity of the RNA samples using spectrophotometer scan in the ultraviolet region and ethidium bromide (EtBr) visualization of intact 18S and 28S RNA bands after agarose gel electrophoresis. Total RNA (0.5 μg) was reverse transcribed using murine leukemia virus reverse transcriptase (50 U) in 1 × polymerase chain reaction (PCR) buffer (50 mM KCl and 10 mM Tris-HCl, pH 8.3), 5 mM $MgCl_2$, 20 U RNase inhibitor, 1 mM each of the dNTPs, and 2.5 μM random hexanucleotide primers. The samples were reverse transcribed for 20 min at 42°C, followed by a 5-min denaturation step at 99°C using a GeneAmp 9600 thermocycler (Perkin Elmer Applied Biosystems, Foster City, CA). We utilized the reverse-transcribed product for PCR amplification using the AmpliTaq DNA polymerase enzyme (2.5 U) and the specific upstream and downstream primers at a concentration of 0.1 μM each. All PCR reagents were purchased from Perkin Elmer. The thermocycler was programmed to cycle at 95°C for a 2-min initial step, at 95°C for 30 sec, and at 68°C for 30 sec, with a final elongation step at 68°C for 7 min. Negative controls for each PCR included a no-template control, where water was added instead of the RNA, and a no-reverse transcriptase control, where water was added instead of the enzyme. Positive controls for MT-3

expression used total RNA from prostate and kidney, where MT-3 is expressed (*12–14*). We removed samples at 25, 30, 35, and 40 PCR cycles to ensure that the reaction remained in the linear region. The final PCR products were electrophoresed on 2% agarose gels containing EtBr along with DNA markers.

RNA isolation and RT-PCR analysis of MT-3 mRNA expression in TCC using paraffin-embedded tissue. Thick sections (10 µm) were cut from formalin-fixed, paraffin-embedded tissue blocks with a microtome. We trimmed the excess paraffin with a sterile blade, then placed the tissue in a 1.5-mL microfuge tube. The tissue was deparaffinized twice at 55°C with xylene for 5 min followed by two washes with 100% ethanol to remove the xylene. We extracted RNA from the deparaffinized tissue using the micro RNA isolation kit (catalog no. 200344; Stratagene, La Jolla, CA). We added 200 µL denaturing buffer containing guanidine isothiocyanate and 1.6 mL β-mercaptoethanol to the sample and vortexed it vigorously. We added 20 µL 2 M sodium acetate (pH 4.0) solution to the samples, along with 220 µL phenol and 60 µL chloroform:isoamyl alcohol. The samples were vortexed and placed on ice for 15 min, followed by centrifugation at maximal speed in a microfuge for 30 min at 4°C to separate the aqueous and organic phase. We transferred the upper aqueous phase to a fresh tube and added 1 µL glycogen (2 µg/µL). RNA was precipitated with the addition of 200 µL ice-cold isopropanol. The samples were left overnight in a -70°C freezer after centrifugation at maximal speed in a microfuge for 30 min at 4°C. The supernatant was removed and the RNA pellet was washed twice with 70% ethanol. The pellet was dried on ice and resuspended in RNase free water.

Total RNA (1 µL) was reverse transcribed in a 20-µL reaction mixture using murine leukemia virus reverse transcriptase (50 U) in 1 × PCR buffer, 5 mM $MgCl_2$, 20 U RNase inhibitor, 1 mM each of the dNTPs, and 2.5 µM random hexanucleotide primers. The samples were reverse transcribed for 20 min at 42°C, followed by a 5-min denaturation step at 99°C using the GeneAmp 9600 thermocycler. The resulting cDNA was amplified in a 100-µL reaction mixture containing 2 mM $MgCl_2$, 1 × PCR buffer, 2.5 U AmpliTaq DNA polymerase, and 0.1 µM of the respective outer primers. We performed the PCR for 30 cycles as follows: 95°C for 30 sec and 68°C for 30 sec, followed by a 7-min final extension step at 68°C. Controls for each PCR included a no-template control in which 1 µL water was added instead of the RNA and a no-reverse transcriptase control in which 1 µL of water was added instead of the enzyme. Five microliters of the product from the first-round of PCR was added to 95 µL of a PCR mixture (2 mM $MgCl_2$, 1 × PCR buffer, 200 µm dNTPs, 2.5 U AmpliTaq DNA polymerase, and 0.1 µM of the respective inner primers) for a second round of PCR. For MT-3, the samples were removed at 18, 20, and 22 cycles, whereas the samples were removed at 30, 35, and 40 PCR cycles for β-actin. We developed the outer and inner nested primers for human β-actin gene and MT-3 using Oligo 5.0 software (Molecular Biology Insights Inc., Cascade, CO). To maintain the MT isoform specificity, the lower outer- and inner-primer sequence for MT-3 was the same according to the Oligo primer analysis program. The sequences of the outer and inner nested primers along with the product sizes for β-actin were as follows: outer primer upper 5′ ATGGATGATGATATCGCCGCG 3′ and lower 5′ CTCCATGTCGTCCCAGTTGGT 3′ (product size: 249 bp), and nested inner primer upper 5′ CGACAACGGCTCCGGCATGT 3′ and lower 5′ TGCCGTGCTCGATGGGGTACT 3′ (product size: 194 bp). The sequences for MT-3 were as follows: outer primer upper 5′ CCGTTCACCGCCTCCAG 3′ and lower 5′CACCAGCCACACTTCACCACA 3′ (product size: 325 bp), and nested inner primer, upper 5′ TCGACATGGACCCTGAGACCT 3′ and lower 5′ CACCAGCCACACTTCACCACA 3′ (product size: 296 bp). The final PCR products were electrophoresed on a 2% agarose gel containing EtBr along with DNA markers (Gibco BRL, Grand Island, NY) to verify the size of PCR products. We determined the intensity (integrated optical density) of the PCR product bands on a Roche Pathology workstation (Autocyte, Burlington, NC) configured with Kontron KS 400 (Zeiss, Thornwood, NY) image analysis software.

Specific cleavage of the MT-3 reaction product used the *Fok*I restriction enzyme. After reverse transcriptase (RT)-PCR (100 µL reaction volume), reaction products were purified using the QiaQuik PCR Purification system (Qiagen, Inc., Valencia, CA) according to the manufacturer's recommended protocol. DNA was eluted into 30 µL TE buffer (10 mM Tris, pH 8.0, 1 mM EDTA). The *Fok*I restriction digestion of MT-3 was carried out by adding NE4 Buffer (New England Biolabs, Beverly, MA), dH_2O, and 10 U *Fok*I enzyme (New England Biolabs) in a final reaction volume of 50 µL to the eluted DNA samples. After incubation at 37°C for 1 hr, we terminated the reaction by adding 5 µL gel-loading buffer. The samples were electrophoresed on a 2% TBE-agarose gel containing 0.5 µg/mL EtBr.

MT-3 protein determination. Bladder tissue samples were homogenized in sodium dodecyl sulfate (SDS) buffer (50 mM Tris, pH 6.8; 2% w/v SDS). Aliquots of 60 µg protein were diluted to 100 µL with buffer consisting of 0.2 M Tris (pH 8.8) and 0.2 M dithiothreitol and heated at 65°C for 15 min to reduce any partially oxidized protein. The samples were centrifuged through a 10-kD molecular weight cutoff centrifuge filter (Micron Separations, Westboro, MA). Volumes of filtrate representing 6 µg protein were diluted to 75 µL with PBS and mixed with an equal volume of 3% glutaraldehyde to enhance detection of MT-3. We applied 100 µL of this mixture (2 µg total protein) to a dot-blot apparatus with a polyvinylidine difluoride membrane. Samples were allowed to flow through the apparatus by gravity, then washed 2 times with PBS. After blocking with 3% bovine serum albumin in PBS, the membrane was soaked in primary antibody (4.5 µg/mL, 1% BSA in PBS) for 2 hr. We washed the membrane 3 times with PBS, and we added alkaline phosphatase-conjugated secondary antibody (Promega, Madison, WI) at a 1:500 dilution. Antibody complexes were visualized using the alkaline phosphatase kit III (Vector Laboratories Inc., Burlingame, CA). We applied standard curves of the conjugated synthetic peptide (Sigma Chemical Co., St. Louis, MO) to each blot. MT-3 protein was quantified by comparing the optical density of the sample dots to the standard MT-3 curve using KS 400 image analysis software. This assay has detection limits in the range of 0.5–2.0 pg MT-3 protein.

Results

Localization and expression of MT-3 in the bladder from controls and patients with IC and related disorders. In previous studies, the human kidney has been shown to be immunoreactive for MT-3 protein and to express both MT-3 mRNA and protein by RT-PCR and Western analysis (*12,13*). For the immunohistochemical analysis of MT-3 expression in the normal bladder, we included sections of human kidney as a positive control during each automated immunohistochemical sequence (Figure 1A). The inclusion of a positive control within each run was especially important in this instance because none of the cell types present in the samples of normal control bladder demonstrated convincing immunoreactivity for MT-3 under identical conditions of analysis (Figure 1B). As compared to a negative control, where MT-3 antibody was deleted from the reaction sequence, MT-3 immunoreactivity in the normal bladder was only nominally, if at all, above background levels (data not shown). This finding is one indication

that the normal human bladder has a very low expression of MT-3. To further define the level of expression of MT-3 in the normal bladder, we isolated total RNA and protein from six samples of control bladder (four females and two males). We used the isolated RNA and proteins to determine the expression of MT-3 mRNA and protein, respectively. The expression of MT-3 mRNA was not detected in any of the six control bladder samples at 35 cycles of nonnested RT-PCR and total RNA inputs of 0.5 μg (Figure 2). These identical total RNA samples yielded strong reaction products for the housekeeping gene, β-actin, at 35 reaction cycles and equal total RNA inputs. As an additional control, we also obtained strong reaction products for MT-3 mRNA from total RNA samples from human kidney at 35 cycles and equal total RNA inputs (Figure 2). Extension of the RT-PCR to 40 cycles failed to produce reaction product for MT-3 in five of the six bladder samples and only a very faint reaction product band was evident in the remaining bladder sample (data not shown). An analysis of MT-3 protein by immunoblot failed to detect the presence of MT-3 protein in any of the six preparations (data not shown). The limit of detection of the assay is approximately 0.5 pg/μg protein. Thus, the analysis of MT-3 expression using total RNA and protein from the human bladder reinforced the immunohistochemical findings regarding MT-3 expression in the normal bladder.

A variety of other nonmalignant disorders of the human bladder that are normally diagnosed by tissue biopsy were examined for the immunoreactivity of MT-3. These included biopsy samples from patients with cystitis, with IC meeting the National Institutes of Health (NIH) research criteria for this disease entity, with symptoms of IC that did not meet all of the NIH criteria, and with symptoms of cystitis after successful BCG therapy for TCC. In all instances, no immunoreactivity for MT-3 was demonstrated in any of the cell types in the bladder (data not shown).

Localization and expression of MT-3 in the bladder from patients with transitional cell carcinoma. In contrast to control urothelium, MT-3 immunoreactivity was demonstrated in LG TCC (Figure 1C), HG TCC (Figure 1D), and in CIS (Figure 1E) of the human bladder. The majority of MT-3 staining within tumors was cytoplasmic. Some tumors, both LG TCCs and HG TCCs, also demonstrated strong nuclear localization (Figure 1F). Several of the samples from each tumor grade also had areas of dysplasia in addition to the carcinoma. In general, although the intensity of MT-3 immunoreactivity within the dysplastic regions was less than that of the corresponding malignant lesion, there were examples within each tumor grade where the staining was of moderate intensity. The MT-3 immunostaining within these dysplastic areas appeared elevated over that of normal urothelium (data not shown). Although present in only a few samples, there was also a tendency for weak MT-3 immunoreactivity within Brunn's nests and in areas of cystitis cystica.

In all cases, MT-3 immunoreactivity was diffuse and was localized to the cytoplasm of the cells and, although variable in intensity among the tumor specimens, all malignant lesions appeared to be immunoreactive for MT-3, albeit a few low-grade lesions only weakly. When the qualitative visual observation of MT-3 immunoreactivity was blinded and quantified as a function of tumor grade, the intensity of MT-3 immunostaining increased as a function of tumor grade (Table 1). When we examined the immunostaining

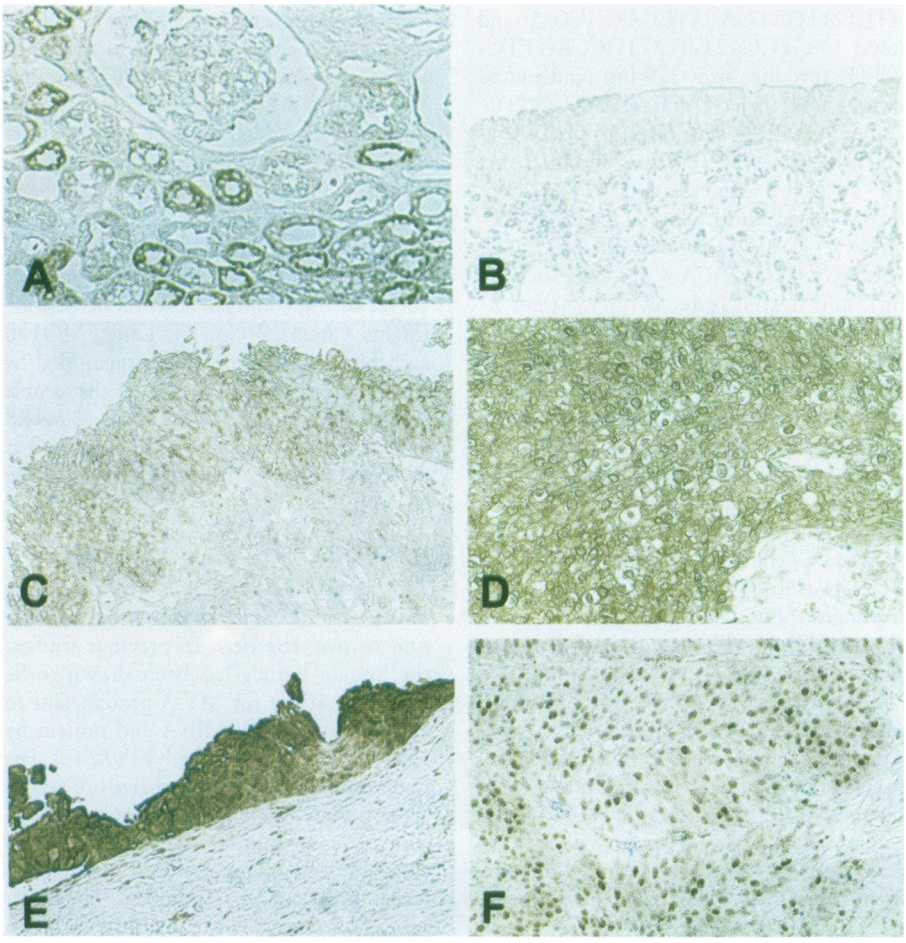

Figure 1. Immunohistochemical analysis of MT-3 expression. (*A*) MT-3 demonstrates heterogeneous staining of the renal tubules, including strong immunoreactivity of the distal tubules. MT-3 dilution (1:100); no counterstain; 200 × magnification. (*B*) Normal urothelium demonstrates negative or very weak immunoreactivity to MT-3. MT-3 dilution (1:100); no counterstain; 200 × magnification. (*C*) LG TCC demonstrates weak to moderate immunoreactivity with MT-3. Similar staining was seen for both invasive and papillary disease. MT-3 dilution (1:100); no counterstain; 200 × magnification. (*D*) HG TCC demonstrates moderate to strong immunoreactivity to MT-3. Similar staining was seen for both invasive and papillary disease. MT-3 dilution (1:100); no counterstain; 200 × magnification. (*E*) CIS of the urinary bladder demonstrates strong immunoreactivity to MT-3. MT-3 dilution (1:100); no counterstain; 200 × magnification. (*F*) Nuclear localization was observed in some urothelial carcinomas. This low-grade papillary urothelial carcinoma demonstrates strong nuclear localization with weak to moderate cytoplasmic immunostaining to MT-3. MT-3 dilution (1:100); no counterstain; 200 × magnification.

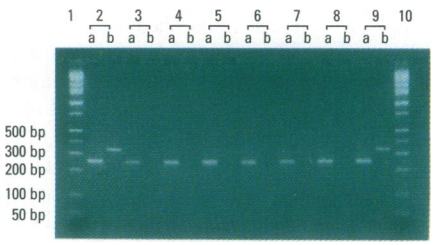

Figure 2. Expression of MT-3 mRNA in control bladder. RT-PCR for β-actin (lane a) and MT-3 (lane b) was performed on two kidney tissue samples (2 and 9) and six control bladder samples (3–8). Lanes 1 and 10 are DNA base pair ladders. The total RNA input was 0.5 μg and the reaction products were removed at 35 cycles.

results for the biologic classes, benign urothelium, dysplastic urothelium, LG-TCC, HG-TCC, and CIS using the Kolmogorov-Smirnov one-sample test and Systat software (SPSS, Inc., Chicago, IL), we found significant differences between all groups (two-sided probability > 0.003). Thus, increased MT-3 immunoreactivity and the malignant phenotype demonstrated a consistent positive correlation in the human bladder.

We determined the expression of MT-3 mRNA by nested RT-PCR in a subset of the samples used for the determination of MT-3 immunoreactivity. We evaluated these full-thickness sections of paraffin-embedded tissue by microscopic examination, and we selected those where the malignant lesion made up > 85% of the tissue sample. This restriction allowed total RNA to be prepared from 16 LG TCCs, 15 HG TCCs, and 5 CISs. In all cases, RT-PCR analysis resulted in a reaction product of the expected number of base pairs (an example for each tumor grade shown in Figure 3). Each sample also expressed β-actin mRNA, a housekeeping gene commonly utilized to control for total RNA integrity and to make comparisons of gene expression patterns by comparison of relative optical densities. In addition, the MT-3 reaction product contains a *Fok*I restriction site not present in any other *MT* gene. An RT-PCR product from each tumor grade was subject to restriction cutting by *Fok*I and in each case we obtained cleavage products of the expected size (e.g., Figure 4). Together, these findings provide supporting evidence that the MT-3 antibody detects MT-3 protein expression in human bladder cancer. The results also demonstrated that the relative expression of the MT-3 reaction product was greater than that of the β-actin housekeeping gene (Table 2). This is based on the relative comparison of the integrated optical densities of the β-actin and MT-3 reaction products. For the 36 samples of bladder cancer, the intensity of the MT-3 RT-PCR product bands was approximately 60% of that of the β-actin housekeeping gene (Table 2). We analyzed the MT-3 reaction products after 22 cycles of nested RT-PCR and we analyzed the β-actin after 35 cycles; this indicates a greater expression of MT-3 mRNA as compared to that of β-actin. This comparison also disclosed that the relative MT-3 mRNA levels were not altered as a function of tumor grade, with all grades having equal relative expressions.

Table 1. MT-3 immunoreactivity in bladder cancer.

Histologic classification	No.	Mean staining intensity	SE	Min	Max
Benign	33	0.58	0.06	0.0	2.0
Dysplasia	18	0.92	0.13	0.5	2.5
Low grade	23	1.29	0.14	0.5	2.5
High grade	25	2.07	0.23	0.25	4.0
CIS	7	2.43	0.30	2.0	4.0

Abbreviations: max, maximum; min, minimum.

Discussion

This study demonstrates that MT-3 is up-regulated in human bladder cancer and that up-regulation increases with increasing tumor grade. However, a mechanistic hypothesis to explain MT-3 overexpression in bladder cancer cannot be proposed because of the limited knowledge regarding the MT-3 member of the *MT* gene family. The MTs are a family of cysteine-rich, low-molecular-weight, intracellular proteins that bind transition metals (*21*). In both mice and humans, there are four classes of similar MT proteins, designated MT-1 through MT-4, defined on the basis of small differences in sequence and charge characteristics (*21–23*). The MT-1 and MT-2 isoforms have been extensively studied and are believed to serve an important role in the homeostasis of essential metals such as Zn^{2+} and Cu^{2+} during growth and development as well as in the detoxification of heavy metals such as Cd^{2+} and Hg^{2+}, rendering the MTs important mediators and attenuators of heavy metal-induced toxicity, particularly hepato- and nephrotoxicity (*21–25*). The MT-1 and MT-2 isoforms exhibit a ubiquitous pattern of tissue expression and are highly inducible by a number of stimuli (*21–24*). In contrast, the MT-3 isoform has been the subject of only limited study. The gene for the MT-3 protein was isolated in 1992; preliminary studies suggested that its expression was limited to neural tissues and that the gene was not metal responsive (*26*). The MT-3 isoform also possesses a unique sequence of eight amino acids that is not present in any other member of the *MT* gene family (*26–28*). Furthermore, in the neural system and derived cell cultures, MT-3 possesses a neuronal cell growth inhibitory activity that is not duplicated by the other human MT classes (*27,29*). This nonduplication of function occurs despite a 63–69% homology in amino acid sequence among MT-3 and the other human MT isoforms. In the neural system, the *N*-terminal region (and not the *C*-terminal sequence of eight unique amino acids) of MT-3 appears to be necessary for its bioactivity and MT-3 bioactivity is not related to metal-binding ability (*30*). The finding that the neuronal expression of MT-3 is associated with the regulation of cell growth allows us to hypothesize that the overexpression of MT-3 in human bladder cancer might also influence the regulation of urothelial cell proliferation. Evidence that the regulation of MT-3 expression in bladder cancer will be complex is suggested by the observation that the levels of MT-3 mRNA and protein expression do not have a direct correlation among the tumor grades. Although there is a progressive increase in MT-3 protein as a function of tumor grade as determined by immunostaining, the level of MT-3 mRNA as determined by RT-PCR remains equal across grades.

The rationale for proposing that MT-3 expression might serve as a biomarker for human bladder cancer is supported by several observations in the present study. First, we found that expression of MT-3 was undetectable using immunohistochemical, western, and RT-PCR techniques in the normal urothelium. MT-3 was also undetectable immunohistochemically in biopsies from other nonmalignant lesions of the bladder, some of which are characterized by increased inflammation. These findings suggest that MT-3 might have the minimal background expression in normal tissue that is necessary for a biomarker that would monitor the effect of agents initiating and promoting the development of bladder cancer. Second, although MT-3 immunoreactivity was increased in all of the bladder cancers examined, the

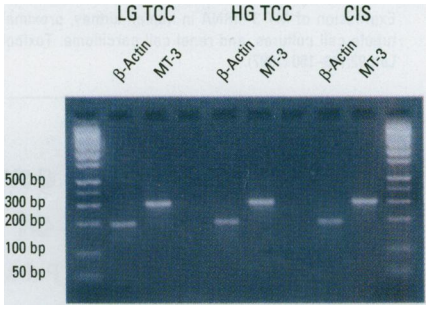

Figure 3. MT-3 expression in bladder cancer. Nested RT-PCR was performed on total RNA isolated from LG TCC, HG TCC, and CIS. Bands representing PCR products for β-actin (194 bp) and MT-3 (296 bp) obtained for each type of carcinoma are shown. Lanes 1 and 10 are DNA ladders.

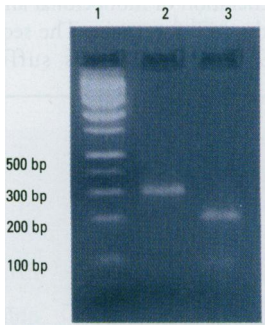

Figure 4. *Fok*I cleavage of nested MT-3 RT-PCR product from total RNA derived from a section of paraffin-embedded bladder cancer. Lane 1, DNA base pair ladder; lane 2, undigested product (296 bp); lane 3, digested product (222 and 74 bp).

Table 2. MT-3 mRNA expression in bladder cancer.

Histologic classification	IOD β-actin[a] Mean ± SE	IOD β-actin[a] Min–max	IOD MT-3[b] Mean ± SE	IOD MT-3[b] Min–max	Relative IOD MT-3/β-actin ratio mean ± SE
Low grade, $n = 16$	14,204 ± 736	8,366–17,746	8,799 ± 1,070	3,212–19,720	0.64 ± 0.08
High grade, $n = 15$	13,597 ± 173	6,902–16,784	7,487 ± 746	3,705–12,825	0.57 ± 0.06
CIS, $n = 5$	13,559 ± 1,883	6,902–17,030	7,758 ± 1,635	4,322–13,858	0.63 ± 0.16

Abbreviations: IOD, integrated optical density; max, maximum; min, minimum.
[a]β-Actin at 35 cycles of nested RT-PCR. [b]MT-3 at 22 cycles of nested RT-PCR.

immunoreactivity was greatest in CIS. This is important because improvements in the treatment of superficial bladder cancer have had a great impact on disease progression. As reviewed by Lamm (*1*), BCG immunotherapy has radically changed the management of CIS. Before 1983, 54% of patients with CIS developed muscle-invasive disease within 5 years. However, with the advent of BCG therapy, 70% or more patients had a complete response, and 65% of complete responders remained disease free for 5 years. With improved BCG maintenance schedules, these numbers are now at 83 and 80%, respectively. Unlike other cancers, CIS of the bladder is a highly malignant, aggressive neoplasm. Thus, a biomarker to detect bladder cancer in its earliest stage, when the lesion is still superficial, has the potential to have a large impact on preventing disease progression. Lastly, the characteristics of both the MT-3 protein and the *MT-3* gene sequence are amenable to the development of probes for assays that could be utilized on the urine or bladder washings from individuals potentially exposed to environmental or occupational agents that are bladder carcinogens. The eight-amino-acid sequence used to raise the present antibody is unique among the members of the *MT* gene family and, based on the current results, appears to have good antigenicity for raising an antibody of high titer and specificity. This would be necessary to extend the current finding to the development of an immunoassay for MT-3 that could be used in large-scale screening protocols. This unique sequence should also allow the generation of monoclonal antibodies against the MT-3 protein. The sequence of the *MT-3* gene also has sufficient sequence divergence in the 5′ and 3′ untranslated regions to develop specific primers for the RT-PCR analysis of MT-3 mRNA. Although probably not applicable to large-scale screening protocols, such reagents could be useful in monitoring for the presence of malignant cells in bladder washings from individuals with a disease history.

References and Notes

1. Lamm DL. Bladder cancer: twenty years of progress and the challenges that remain. CA Cancer J Clin 48:263–268 (1998).
2. Droller MJ. Bladder cancer: state-of-the-art care. CA Cancer J Clin 48:269–284 (1998).
3. Landis SH, Murray T, Bolden S, Wingo PA. Cancer statistics. CA Cancer J Clin 49:8–31 (1999).
4. Catalona WJ. Urothelial tumors of the urinary tract. In: Campbell's Urology (Walsh PC, Retik AB, Stanley TA, Vaughan ED Jr, eds). Philadelphia:WB Saunders Co, 1992;1094–1158.
5. Whitmore WF Jr. Toward the rational management of bladder cancer: an overview. Urology 31:5–8 (1988).
6. Rehn L. Blasengeschwulte bei fuchsin-arbeitern. Arch Klin Chir 50:588 (1895).
7. Hueper WC, Wiley FH, Wolfe HD. Experimental production of bladder tumors in dogs by administration of beta-naphthylamine. Hyg Toxicol 20:46 (1938).
8. Case RAM, Hosker ME, McDonald DB, Pearson JT. Tumours of the urinary bladder in workmen engaged in the manufacture and use of certain dyestuff intermediates in the British chemical industry. Br J Ind Med 11:75–104 (1954).
9. Morrison AS, Buring JE, Verhoeck WG, Aoki K, Leck I, Ohno Y, Obata K. An international study of smoking and bladder cancer. J Urol 131:650–654 (1984).
10. Clavel J, Cordier S, Boccon-Gibod L, Hemon D. Tobacco and bladder cancer in males: increased risk for inhalers and smokers of black tobacco. Int J Cancer 44:605–610 (1989).
11. Vincis P, Esteve J, Hartge P, Hoover R, Silverman DT, Terracini B. Effects of timing and type of tobacco in cigarette-induced bladder cancer. Cancer Res 48:3849–3852 (1998).
12. Hoey JG, Garrett SH, Sens MA, Todd JH, Sens DA. Expression of MT-3 mRNA in human kidney, proximal tubule cell cultures, and renal cell carcinoma. Toxicol Lett 92:149–160 (1997).
13. Garrett SH, Sens MA, Todd JH, Somji S, Sens DA. Expression of MT-3 protein in the human kidney. Toxicol Lett 105:207–214 (1999).
14. Garrett SH, Sens MA, Shukla D, Nestor, S, Somji S, Todd JH, Sens DA. Metallothionein isoform 3 expression in the human prostate and cancer-derived cell lines. Prostate 41:196–202 (1999).
15. Palmiter RD, Findley SD, Whitmore TE, Durnam DM. MT-III, a brain-specific member of the metallothionein gene family. Proc Natl Acad Sci USA 89:6333–6337 (1992).
16. Somji S, Garrett SH, Sens DA, Nseyo UO, Todd JH, Sens MA. Expression of heat shock protein 27 in human bladder. Urol Pathol 9:1-15 (1998).
17. Somji S, Sens DA, Todd JH, Garrett SH, Nseyo UO, Sens MA. Expression of heat shock protein 70 in the bladder from controls and patients with interstitial cystitis-like syndromes. Urol Pathol 10:9–21 (1999).
18. Somji S, Sens DA, Todd JH, Garrett SH, Nseyo UO, Sens MA. The expression of heat shock protein 60 is reduced in the bladder of patients with interstitial cystitis. Urol Pathol 10:97–108 (1999).
19. Mididoddi S, McGuirt JP, Sens MA, Todd JH, Sens DA. Isoform-specific expression of metallothionein mRNA in the developing and adult human kidney. Toxicol Lett 685:17–27 (1996).
20. Friedline JA, Garrett SH, Somji S, Todd JH, Sens DA. Differential expression of the MT-1E gene in estrogen receptor positive and negative human breast cancer cell lines. Am J Pathol 152:23–28 (1998).
21. Hamer DH. Metallothionein. Annu Rev Biochem 55:913–951 (1986).
22. Cousins RJ. Metallothionein: aspects related to copper and zinc metabolism. J Inherited Metab Dis 6:15–21 (1983).
23. Kägi JHR. Evolution, structure and chemical activity of class I metallothioneins: an overview. In: Metallothionein III. Biological Roles and Medical Implications (Suzuki KT, Imura N, Kimura M, eds). Berlin:Birkhauser Verlag, 1993;29–56.
24. Kagi JHR, Hunziker P. Mammalian metallothionein. Biol Trace Element Res 21:111–118 (1989).
25. Goering PL, Klaassen CD. Altered subcellular distribution of cadmium following cadmium pretreatment: possible mechanism of tolerance to cadmium-induced lethality. Toxicol Appl Pharmacol 70:195–203 (1983).
26. Palmiter RD, Findley SD, Whitmore TE, Durnam DM. MT-III, a brain-specific member of the metallothionein gene family. Proc Natl Acad Sci USA 89:6333–6337 (1992).
27. Uchida Y, Takio K, Titani K, Ihara Y, Tomonaga M. The growth inhibitory factor that is deficient in Alzheimer's disease is a 68 amino acid metallothionein-like protein. Neuron 7:337–347 (1991).
28. Tsuji S, Kobayashi H, Uchida Y, Ihara Y, Miyataka T. Molecular cloning of human growth inhibitory factor cDNA and its down-regulation in Alzheimer's disease. EMBO J 11:4843–4850 (1992).
29. Amoureux M-C, Wurch T, Pauwels PJ. Modulation of metallothionein-III mRNA content and growth rate of rat C6-glial cells by transfection with human 5-HT1D receptor genes. Biochem Biophys Res Comm 214:639–645 (1995).
30. Sewell AK, Jensen LT, Erickson JC, Palmiter RD, Winge DR. The bioactivity of metallothionein-3 correlates with its novel β domain sequence rather than metal binding properties. Biochemistry 34:4740–4747 (1995).